MAJOR ARTICLE

Radiation-Induced Cellular and Molecular Alterations in Asexual Intraerythrocytic *Plasmodium falciparum*

Miranda S. Oakley,[1] Noel Gerald,[2] Vivek Anantharaman,[4] Yamei Gao,[3] Victoria Majam,[2] Babita Mahajan,[2] Phuong Thao Pham,[2] Leda Lotspeich-Cole,[1] Timothy G. Myers,[5] Thomas F. McCutchan,[6] Sheldon L. Morris,[1] L. Aravind,[4] and Sanjai Kumar[2]

[1]Division of Bacterial, Parasitic, and Allergenic Products, [2]Division of Emerging and Transfusion Transmitted Diseases; and [3]Division of Viral Products, Center for Biologics Evaluation and Research, Food and Drug Administration, Rockville; [4]National Center for Biotechnology Information, National Library of Medicine; [5]Microarray Research Facility, Research and Technologies Branch, and [6]Laboratory of Malaria and Vector Research, National Institutes of Health, Bethesda, Maryland

Background. γ-irradiation is commonly used to create attenuation in *Plasmodium* parasites. However, there are no systematic studies on the survival, reversion of virulence, and molecular basis for γ-radiation–induced cell death in malaria parasites.

Methods. The effect of γ-irradiation on the growth of asexual *Plasmodium falciparum* was studied in erythrocyte cultures. Cellular and ultrastructural changes within the parasite were studied by fluorescence and electron microscopy, and genome-wide transcriptional profiling was performed to identify parasite biomarkers of attenuation and cell death.

Results. γ-radiation induced the death of *P. falciparum* in a dose-dependent manner. These parasites had defective mitosis, sparse cytoplasm, fewer ribosomes, disorganized and clumped organelles, and large vacuoles—observations consistent with "distressed" or dying parasites. A total of 185 parasite genes were transcriptionally altered in response to γ-irradiation (45.9% upregulated, 54.1% downregulated). Loss of parasite survival was correlated with the downregulation of genes encoding translation factors and with upregulation of genes associated with messenger RNA–sequestering stress granules. Genes pertaining to cell-surface interactions, host-cell remodeling, and secreted proteins were also altered.

Conclusions. These studies provide a framework to assess the safety of γ-irradiation attenuation and promising targets for genetic deletion to produce whole parasite-based attenuated vaccines.

Keywords. NOD2; IL-17; Th17; T lymphocytes; ocular toxoplasmosis; Toxoplasma gondii.

Exposure to ionizing radiation has a profound effect on the viability and further replication of living cells. Radiation is used for the treatment of cancer [1], generation of attenuated vaccines [2], and in food safety [3]. Radiation attenuation has also been one of the earliest methods used to generate whole parasite–based malaria vaccines [4–6]. Given the importance of ionizing radiation in the treatment of different forms of cancer, a large body of scientific data has accumulated on the effects of ionizing radiation on the cell cycle [7]. Such studies have shed light on the molecular and biochemical aspects of radiation-mediated cell death and survival mechanisms [1, 8]. These studies have also provided insight into the cell cycle checkpoints and the complex signaling pathways and associated molecules that ensure that each phase of the cell cycle is completed without errors [7, 9, 10].

Ionizing radiation is detrimental to the growth and survival of *Plasmodium* parasites. In murine models, asexual blood-stage parasites exposed to high doses of radiation failed to cause blood-stage parasite infection [11], and immunization with radiation-attenuated asexual-stage parasites protected against parasitemia [11–13] and

Received 11 May 2012; accepted 8 August 2012; electronically published 24 October 2012.

Correspondence: Sanjai Kumar, PhD, CBER, FDA, 5516 Nicholson Ln, Kensington, MD 20895 (sanjai.kumar@fda.hhs.gov).

The Journal of Infectious Diseases 2013;207:164–74
Published by Oxford University Press on behalf of the Infectious Diseases Society of America 2012.
DOI: 10.1093/infdis/jis645

experimental cerebral malaria [11]. In preerythrocytic-stage malaria, exposure of *Plasmodium* sporozoites to a threshold level of γ-radiation allows their invasion into liver cells and early development. However, these parasites undergo arrested development and fail to produce infectious liver-stage merozoites and, consequently, blood-stage parasite infection [14]. Irradiation-attenuated malaria sporozoites protect mice [4, 15] and humans [5, 16] against malaria in experimental challenge studies. Accordingly, despite the limited success of subunit-based malaria vaccines in clinical testing [17], there has been considerable interest in using radiation exposure to create an attenuated sporozoite-stage vaccine [14, 16].

In this study, we measured the effects of different doses of γ-irradiation on *P. falciparum* in short-term and long-term cultures. These studies were performed to evaluate both the immediate effect on survival and the ability of rare parasite populations to recover and repopulate. We also studied the effect of γ-irradiation on parasite structure, by fluorescence microscopy and transmission electron microscopy. In addition, we performed extensive genome-wide transcriptional profiling in *P. falciparum* exposed to increasing doses of γ-radiation, to identify parasite proteins that could be correlated with survival and cell death, and, on the basis of the data set, created a functionally diverse molecular signature of growth attenuation. Last, bioinformatic analyses were performed to decipher the biological systems altered by γ-irradiation that are associated with growth regulation and survival.

MATERIALS AND METHODS

Parasite Cultivation, γ-Irradiation Treatment of Parasites, and Parasite Survival and Growth Studies

Cultivation, γ-irradiation treatment, and survival and growth studies of *P. falciparum* were performed as described in the Supplementary Materials.

Fluorescence Microscopy and Transmission Electron Microscopy Studies

Detailed procedures for immunofluorescence and electron microscopy studies to determine the effect of γ-radiation–induced ultrastructural changes in parasites are provided in the Supplementary Materials.

Preparation of RNA and Microarray Expression Analysis

RNA preparation and microarray analysis of untreated and γ-radiation–treated parasites were performed as previously described [18]. Details of these procedures can be found in the Supplementary Materials.

Gene Annotation, Ontology, and Bioinformatic Analyses

Details of gene annotation, ontology, and bioinformatic analyses to determine the biological pathways associated with γ-radiation–induced growth attenuation and cell death can be found as described earlier [18–20] and in the materials and methods and results sections of the Supplementary Materials.

Real-Time Polymerase Chain Reaction (PCR)

Real-time PCR to create a molecular signature of γ-radiation–induced growth attenuation of *P. falciparum* was performed as previously described [20]. A further description can also be found in the Supplementary Materials.

Statistical Analysis

We used logistic regression to analyze the effect of γ-irradiation on nuclear division and microneme development in asexual blood-stage *P. falciparum*. The adjacent categorical model was used to assess the cell cycle progression on the basis of the number of nuclei counted during schizogony in γ-radiation–treated and untreated *P. falciparum* cultures. The logit model was used to measure the effect of γ-radiation treatment on microneme development by comparing the percentage of RAP1- and EBA175-positive parasites between the treated and untreated *P. falciparum* cultures.

RESULTS

Effect of γ-Irradiation on the Survival and Growth of *P. falciparum*

Duplicate in vitro cultures of asynchronous parasites at 0.5% initial parasitemia were treated with 15, 30, and 60 K of γ-radiation (where K is equal to 1 kilorad of γ-radiation delivered by a Cesium-137 source), and parasitemia was then monitored every 24 hours for 3 days. Parasitemia continued to be monitored on days 7 and 13 in the group treated with 60 K of γ-radiation.

In untreated control cultures, parasitemia increased from 0.5% to 0.73% ± 0.15% and 6.20% ± 0.30%, after 24 and 48 hours, respectively, and then slightly dropped to 4.78% ± 0.32% after 72 hours of culture, an indication of culture overgrowth. Treatment with γ-irradiation resulted in a dose-dependent decrease in parasite growth and survival that was most evident at 48 and 72 hours after treatment. In cultures treated with 15 K of γ-radiation, while parasitemia remained unchanged during the initial 24 hours after treatment, parasite survival was markedly reduced by 84% and 73% at 48 and 72 hours, respectively, after treatment. The detrimental effect of γ-irradiation on parasite survival was even more dramatic at higher doses. Parasitemia was reduced by 13%, 91%, and 95% at 24, 48, and 72 hours, respectively, after treatment with 30 K of γ-radiation and by 29%, 93%, and 99.5% at 24, 48, and 72 hours, respectively, after treatment with 60 K of γ-irradiation (Figure 1).

To evaluate the ability of rare parasite populations to recover and repopulate, cultures treated with 60 K of γ-radiation were monitored for long-term parasite growth and

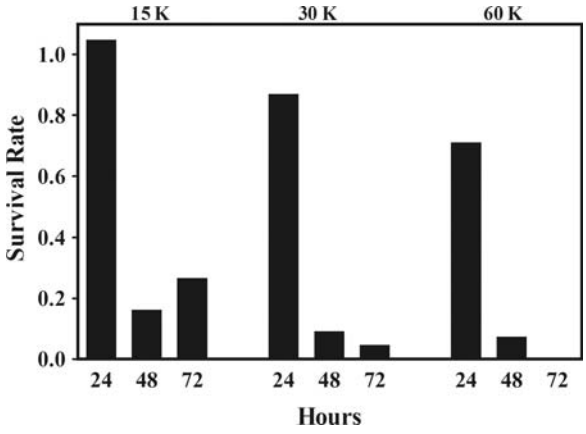

Figure 1. Effect of incremental doses of γ-irradiation on the survival of asexual erythrocytic-stage asynchronous cultures of *Plasmodium falciparum*. Parasite survival is expressed as the number of parasites in γ-radiation–treated cultures divided by the number of parasites in untreated cultures and was determined over a period of 72 hours. Abbreviation: K, kilorad of γ-radiation delivered by a Cesium-137 source.

survival. After 7 days of continuous culture, parasitemia continued to drop from 0.23% (at 72 hours) to 0.099% (at day 7) but by day 13 rose to 1.27% and thereafter continued to grow at a rate that was indistinguishable from that of untreated control cultures.

Morphology of Irradiated Parasites, by Fluorescence Microscopy

To better understand the cellular effects of ionizing radiation on the asexual blood-stage of *P. falciparum*, we magnetically enriched parasites from both irradiated (60 K) and nonirradiated control samples after 24 hours of culture and observed parasite organelles by fluorescence microscopy. We assessed the development and structural integrity of parasite nuclei, rhoptries, and micronemes.

In control cultures, 40% of the parasites (230 of 579) contained 1–4 nuclei, 33% (193 of 579) contained 5–8 nuclei, and 27% (156 of 579) contained ≥9 nuclei (Figure 2*A*). This distribution is typical for an unsynchronized blood-stage culture and indicated that the parasites were progressing through the multinuclear cycle of asexual development. In advanced schizonts from control cultures, the nuclei were sharply defined, condensed, and arranged in an orderly pattern around the parasite (Figure 2*B* and 2*D*).

In contrast to control cultures, irradiated cultures had fewer clearly distinguishable nuclei per parasite: 84% of irradiated parasites (569 of 675) contained 1–4 nuclei, 13% (88 of 675) contained 5–8 nuclei, and only 3% (18 of 675) contained ≥9 nuclei (Figure 2*A*). This distribution indicated that the irradiated parasite culture was not progressing through multinuclear development normally. In irradiated parasites, the nuclei often appeared to be clumped together in the cytoplasm and in some examples presented irregular shapes or sizes (Figure 2*C* and 2*E*). Furthermore, statistical analysis by adjacent categorical modeling predicted that, overall, irradiated parasites had an approximately 5-fold higher prospect of having fewer number of multinucleated *P. falciparum* schizonts, compared with untreated parasites.

We also evaluated development of blood-stage parasites by examining the morphology of rhoptries and micronemes, the vesicular organelles that develop during schizogony and that ultimately form part of the apical complex in daughter merozoites. Both organelles are important for establishing a new parasitophorous vacuole when the merozoite invades a new red blood cell [21]. The rhoptry-associated protein 1 (RAP1) is a rhoptry component that appears in vesicles during the third nuclear division of schizogony and that remains visible as the parasites progress through asexual blood-stage development [22]. In control cultures, 66% of the parasites (162 of 246) were positive for RAP1, and as expected, these RAP1-positive parasites contained at least 5 nuclei, and half of these parasites were more advanced schizonts containing ≥9 nuclei. As reported in other studies, the RAP1 vesicles in control parasites were arranged in a regular pattern around the nuclei (Figure 2*B*). In contrast to control parasites, only 18% of irradiated parasites (56 of 319) stained positively for RAP1. Approximately half of the RAP1-positive irradiated parasites contained 5–8 nuclei, yet half of the RAP1 positive parasites appeared to only contain 1–4 nuclei. Thus, the irradiated cultures had fewer RAP1-positive parasites than control cultures, and the RAP1-positive parasites from irradiated cultures appeared to have fewer nuclei, on average, than RAP1-positive parasites from control cultures. The RAP1 vesicles in irradiated parasites were sometimes clumped together, and some of these RAP1 structures appeared to be abnormally large (Figure 2*C*).

Micronemes can be detected in late-stage schizonts after the fourth nuclear division by the appearance of the protein EBA175 in these structures [22]. In control cultures, 16% of the parasites (30 of 192) were positive for EBA175. EBA175 staining was visible as a ring around each nucleus, and the staining usually included a brighter spot at one end of the nucleus (Figure 2*D*). Consistent with previous reports, most of the EBA175-positive parasites in control cultures contained ≥9 nuclei and showed evidence of daughter cell budding, one of the final steps of blood-stage development. In irradiated cultures, only 7% of the parasites (17 of 230) were EBA175 positive, and the majority of these parasites contained only 5–8 nuclei. Similar to the observations with RAP1 staining, irradiated cultures had fewer EBA175-positive parasites than control cultures, and the EBA175-positive parasites from irradiated cultures appeared to have fewer nuclei than those from control cultures. The EBA175 staining in these irradiated

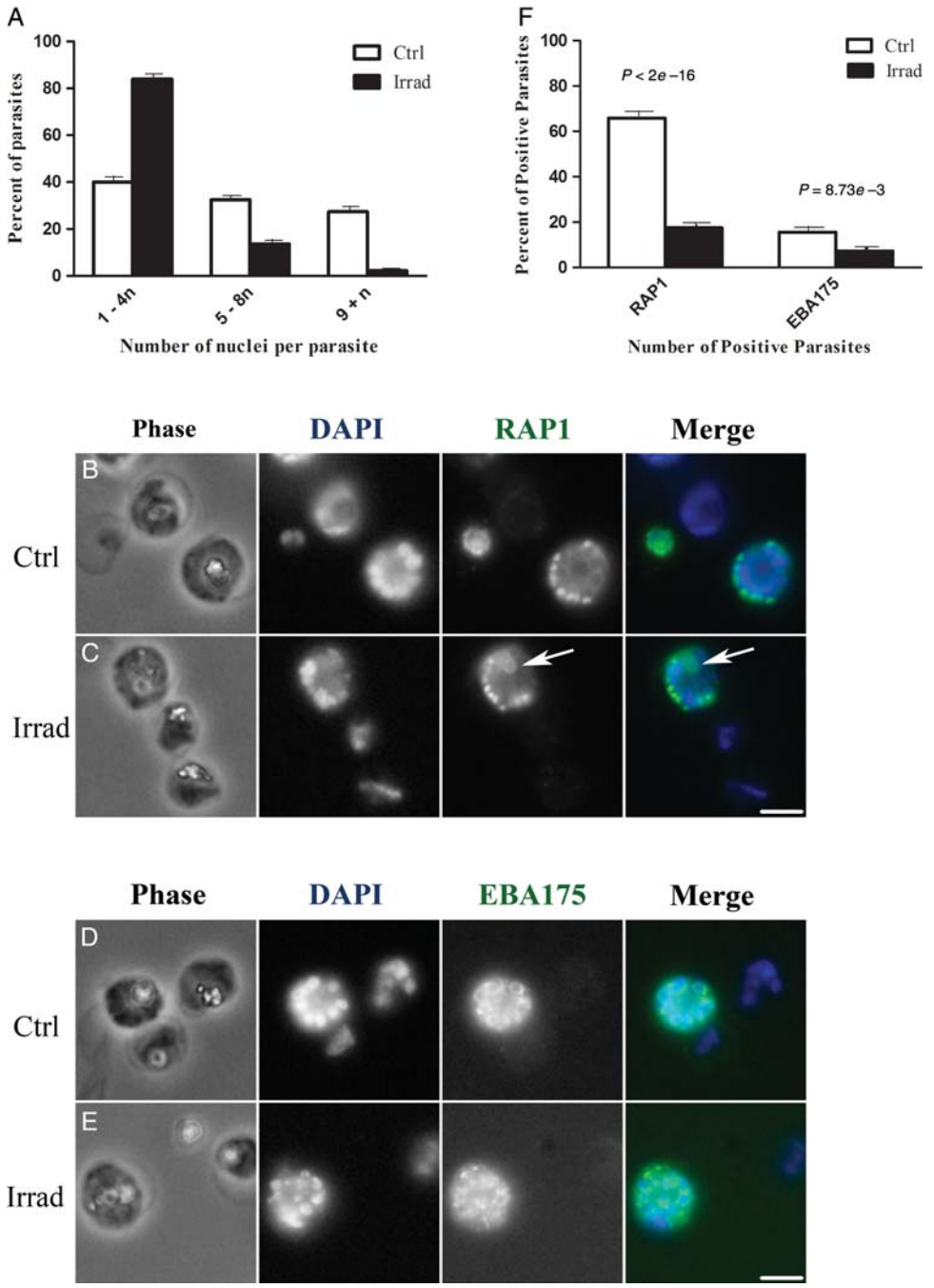

Figure 2. Fluorescence microscopy of purified blood-stage *Plasmodium falciparum* parasites from irradiated (Irrad) and control (Ctrl) cultures. *A*, Quantification of the number of nuclei per parasite. DAPI-stained nuclei were visually counted in approximately 600 parasites per group. In control cultures (white bars), 40%, 33%, and 27% of the parasites contained 1–4, 5–8, and ≥9 nuclei, respectively. This indicated that the parasites were developing through the entire asexual blood-stage cycle. In irradiated cultures (black bars), 84% of the parasites contained 1–4 nuclei and only 3% contained ≥9 nuclei, indicating that blood-stage parasite development was impeded. *B–E*, Parasite morphology is shown with phase contrast microscopy (Phase). Nuclei are labeled with DAPI (blue in merged color images), rhoptries are labeled with anti-RAP1 antibody (green in merged image), and micronemes are labeled with anti-EBA175 antibody (green in merged image). *B*, In control cultures, anti-RAP1 antibody stains developing rhoptries in mid-to-late schizonts. A total of 66% of control parasites (162 of 246) contain RAP1-positive vesicles that are arranged in an organized fashion around the nuclei. *C*, In irradiated cultures, only 18% of the parasites (56 of 319) were positive for RAP1 staining, and the RAP1 structures were sometimes clumped or had distorted morphologies (arrow). *D*, In control cultures, anti-EBA175 antibody stains developing micronemes in late-stage schizonts (16% of the parasites [30 of 192]), appearing as a ring around the nuclei with a brightly staining section on one side. *E*, In irradiated cultures, only 7% of the parasites (17 of 230) were EBA175 positive, and the stained structures were arranged in irregular patterns around the cell. *F*, The overall percentage of RAP1-positive and EBA 175–positive *P. falciparum* parasites in control and irradiated cultures. Scale bar = 4 microns.

parasites was generally disorganized and not always associated with budding parasites (Figure 2*E*, EBA175), indicating a disruption in microneme development and schizont development overall in irradiated cultures. The logit model yielded a *P* value of $<2 \times 10^{-16}$ for RAP1-positive parasites and a *P* value of 8.73×10^{-3} for EBA175-positive parasites, indicating that irradiation treatment interfered with organogenesis and development of *P. falciparum* (Figure 2*F*).

Morphology of Irradiated Parasites, by Electron Microscopy

To further investigate the cellular effects of radiation on blood-stage parasites, magnetically enriched control parasites and 60 K–irradiated parasites were observed by thin section electron microscopy after 24 hours of culture (Figure 3). In the majority of control parasites (56 of 58), the cytoplasm was densely packed with ribosomes, and membranous organelles with distinct outlines were distributed around the cell, with an ordered structure (Figure 3*A* and 3*C*). In irradiated cultures, 49% of the parasites (36 of 73) had an abnormal appearance that included sparse cytoplasms with few ribosomes, disorganized and clumped organelles, and, in some cases, abnormally large vacuoles (Figure 3*B* and 3*D*). These attributes are consistent with distressed or dying cells. However, in the abnormal parasites from irradiated cultures, the parasite

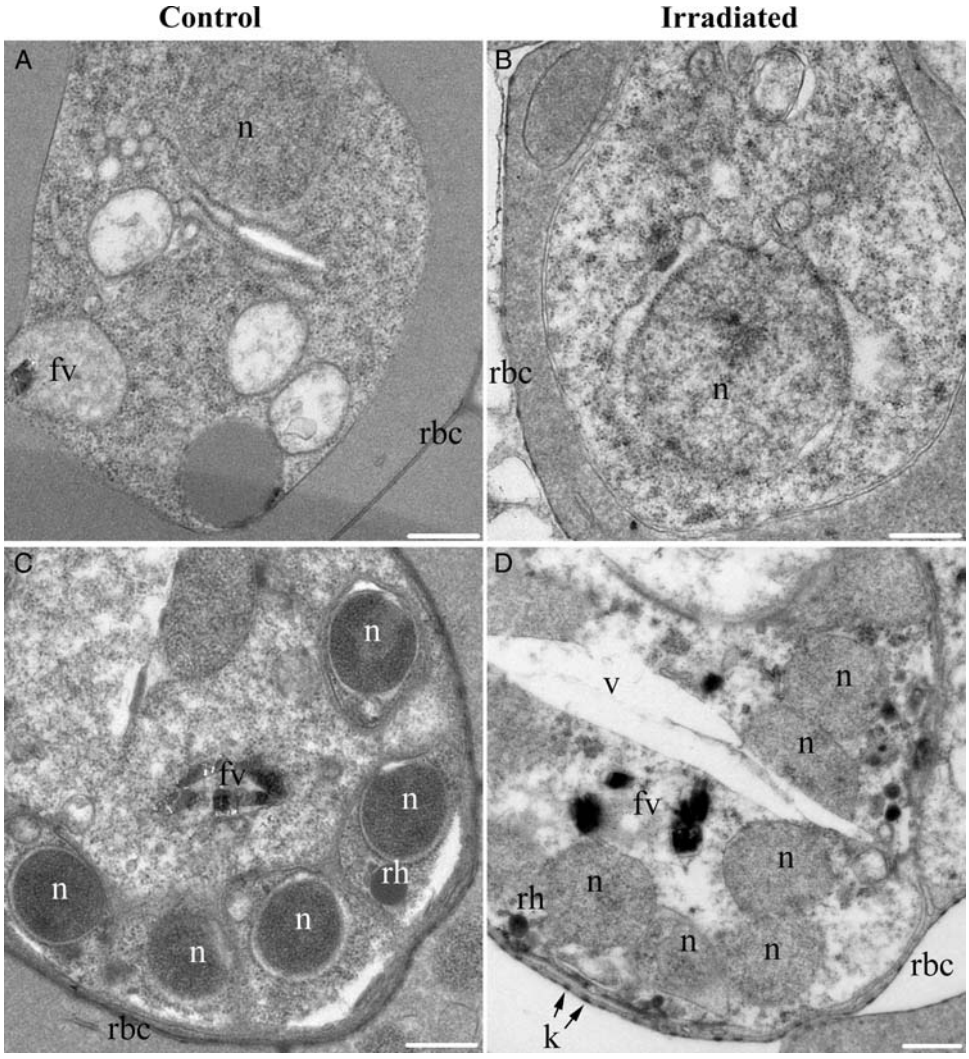

Figure 3. Thin-section electron microscopy of purified blood-stage *Plasmodium falciparum* parasites from control and irradiated cultures. Examples of trophozoite (*A* and *B*) and late schizont (*C* and *D*) parasites are shown as judged from the size and number of parasite nuclei and the size of the parasite inside the host cell. *A* and *C*, In control cultures, the majority of the parasites (56 of 58) displayed organized internal structures and their cytoplasms were densely packed with ribosomes and organelles. *B* and *D*, In irradiated cultures, 49% of parasites (36 of 73) displayed abnormal morphologies that included sparse cytoplasms, clumped organelles, abnormally large vacuoles, and generally disorganized structure. Parasite plasma membrane, parasitophorous vacuole membrane, and host red blood cell plasma membrane (rbc) appeared to be intact in irradiated samples. Scale bar = 500 nm. Abbreviations: fv, food vacuole; k, knob; n, nucleus; rh, rhoptry; v, abnormal vacuole.

Table 1. γ-Radiation–Induced Alterations in the *Plasmodium falciparum* Genome, by Biological Functions of Associated Proteins

	No. of Proteins, by γ-Radiation Dose					
	15 K		30 K		60 K	
Biological Function	Downregulation	Upregulation	Downregulation	Upregulation	Downregulation	Upregulation
Chaperone/protein stability	1		1	1	1	
Cytoskeleton	1	2	1	4		
Chromatin	1	1	3		1	1
DNA metabolism			5			
RNA metabolism		2	2	3	1	
Ubiquitin	1		4	1	1	1
Transcription		1		1	1	
Translation	3		9		5	
Protein processing	1			1		
Signal transduction	1		5	2	2	2
Metabolism	1		5	3		1
Surface/exported protein	3	4	19	20	5	7
Trafficking		1	1	2		
Transport	2		2			
Miscellaneous		2	7	4	1	1
Plasmodium only	3	3	9	2	3	2
Non–protein-coding transcripts	4	6	4	4	2	
Total	22	22	77	48[a]	23[b]	15

Abbreviation: K, kilorad of γ-radiation delivered by a Cesium-137 source.

[a] PF11_0330 has been counted in 2 categories: RNA metabolism and Ubiquitin.

[b] PFL1350w has been counted in 2 categories: RNA metabolism and Translation.

plasma membrane, the parasitophorous vacuole membrane, and the host red blood cell plasma membrane all appeared to be intact.

γ-Radiation–Induced Alterations in the Expression Profile of *P. falciparum*

To elucidate the molecular mechanism of γ-radiation–induced attenuation of parasite growth and survival, microarray analysis was performed in duplicate on RNA isolated from nonirradiated (0 K) versus γ-radiation–treated (15, 30, 60 K) parasite cultures at 3% initial parasitemia. The criterion for altered gene expression in an individual gene induced by γ-irradiation was a statistically significant ($P<.05$, by 2-tailed Student t test) ≥2-fold increase (upregulation) or decrease (downregulation) in the average ratio of expression between nonirradiated and γ-irradiated cultures.

A total of 185 genes were transcriptionally altered in response to treatment with 15, 30, or 60 K of γ-radiation, with some overlap in gene expression between doses of γ-radiation (Table 1). Of these 185 genes, 85 (45.9%) were upregulated, and 100 (54.1%) were downregulated. This data set of 185 genes with statistically significant findings provides a platform for dissecting the molecular mechanism(s) of γ-radiation–induced attenuation of parasite growth and survival. Additional data can be found in the results section of the Supplementary Materials.

Biological Characteristics of γ-Radiation–Regulated Genes

Next, we systematically categorized these 185 transcriptionally altered genes by function to further decipher the biological consequences of γ-irradiation on *P. falciparum*. A description of some of the biologically relevant pathways altered in response to γ-irradiation is provided below.

A Systemic Slowdown of Translation by Irradiation

Our previous study of the response of *P. falciparum* to an unrelated stress, febrile temperature, presented evidence for a major downregulation of translation related genes, including those encoding ribosomal proteins [18]. Interestingly, in the current study, at least 8 ribosomal proteins, 1 ribosome assembly GTPase (PFE1435c, Nug1 ortholog), and 1 ribosomal RNA-modifying pseudouridylate synthase were significantly downregulated by irradiation (Tables 1 and 2). In contrast, only 1 gene encoding a protein involved in ribosomal biogenesis, the Nop52 ortholog (PFI1510w), was upregulated by irradiation.

Effect of γ-Irradiation on DNA Repair and Attenuation of Replication-Related Functions

Five of the 185 parasite genes (<3% of the genes) showing altered expression in response to radiation are directly related

Table 2. Biologic Functions of Proteins Expressed by a Subset of *Plasmodium falciparum* Genes From Our Data Set That Are Regulated by γ-Irradiation

Protein, by Biological Function	Gene(s)	Regulation Direction, by Radiation Dose[a]
Chaperone/protein stability		
DNAJ chaperone protein	*PFI0985c*	↓ 15 K
AAA ATPase	*PFI0355c*	↓ 30, 60 K
AAA Atpase; Pch2p like	*PF11_0405*	↑ 30 K
Cytoskeleton		
Kinesin	*PFL2190c*	↓ 15 K
SF-assemblin with fibrinogen domain	*PF14_0311*	↓ 30 K
Fibrinogen	*PF11_0388*	↑ 15 K
WD40 repeat containing membrane-associated protein	*PF10_0371*	↑ 15 K
Kinesin	*PFL0545w*	↑ 30 K
STOP repeat protein involved in microtubule stabilization	*PFI0460w*	↑ 30 K
Dyenin beta chain	*PF14_0626*	↑ 30 K
Radial spoke protein	*PFL0760w*	↑ 30 K
Chromatin		
SWIRM and MYB containing protein Rsc8	*PFL1215c*	↓ 15, 30, 60 K
PHD and ELM2 domain containing protein	*PF11_0429*	↓ 30 K
NOT1	*PF14_0170*	↓ 30 K
NOT2	*PF11_0297*	↑ 60 K
SWC5	*PFE0275w*	↑ 15 K
DNA metabolism		
DNA replication complex GINS protein PSF1	*PFE1175w*	↓ 30 K
Origin recognition complex subunit 2	*MAL7P1.21*	↓ 30 K
BRCT and DNA polymerase containing protein Rev1	*PFI0510c*	↓ 30 K
DNA topoisomerase II	*PF14_0316*	↓ 30 K
RP-A-like OB-fold nucleic acid binding domain	*PF11_0332*	↓ 30 K
RNA metabolism		
RNase III	*PF11_0300*	↓ 30 K
C2H2-containing protein	*PFL2075c*	↓ 30 K
RNA pseudouridylate synthase	*PFL1350w*	↓ 60 K
Nop52 (Nop52/Rrp1p/NNP-1 family)	*PFI1510w*	↑ 15 K
FHA and RRM containing protein	*PF11_0347*	↑ 15, 30 K
LSM12 with SM and anticodon-binding domain	*PFF0580w*	↑ 30 K
RRM and RING containing protein	*PF11_0330*	↑ 30 K
Ubiquitin and proteasome		
OTU cysteine protease	*PFI1135c*	↓ 15, 60 K
Cysteine proteinases ULP1	*PFL1635w*	↓ 30 K
MATH domain containing protein	*PFI1065c*	↓ 30 K
FBOX and LRR domain containing protein	*PFF0710w*	↓ 30 K
26S proteasome AAA-ATPase subunit RPT3	*PFD0665c*	↓ 30 K
RRM and RING containing protein	*PF11_0330*	↑ 30 K
RING finger	*PFC0610c*	↑ 60 K
Transcription		
Transcription factor with AP2 domain	*MAL8P1.153*	↓ 60 K
Transcription factor with AP2 domain	*PF14_0271*	↑ 15, 30 K
Translation		
40S ribosomal protein S3A	*MAL3P7.35*	↓ 30 K
40S ribosomal protein S7	*PF13_0014*	↓ 15, 30, 60 K
40S ribosomal protein S12	*MAL3P2.28*	↓ 30, 60 K
40S ribosomal protein S15	*MAL13P1.92*	↓ 30 K
40S ribosomal protein S18	*PF11_0272*	↓ 30 K
40S ribosomal protein S20e	*PF10_0038*	↓ 15, 30 K
60S ribosomal protein L7	*MAL3P2.29*	↓ 30 K
60S ribosomal protein L21e	*PF14_0240*	↓ 30, 60 K
Methionine aminopeptidase	*MAL8P1.140*	↓ 30 K
Nug1, nuclear ribosome–associated GTPase	*PFE1435c*	↓ 60 K
RNA pseudouridylate synthase	*PFL1350w*	↓ 60 K
Protein processing		
Rhomboid protease (2)	*PFF0900c, MAL8P1.16*	↓ 15 (1) K; ↑ 30 (1) K
Signal transduction		
Inositol hexakisphosphate kinase	*PF13_0089*	↓ 15, 30, 60 K
Inositol polyphosphate kinase (synaptojanin)	*PF07_0024*	↓ 30, 60 K
S/T/Y kinase	*MAL7P1.18*	↓ 30 K
Protein kinase	*PFI0160w*	↓ 30 K
FIKK family S/T/Y kinase	*PFI0100c*	↓ 30 K
cAMP-specific 3′,5′-cyclic phosphodiesterase 4B	*MAL13P1.119*	↑ 30 K
PTPA serine/threonine-protein phosphatase	*PF14_0280*	↑ 30 K
PP2A	*PFI1245c*	↑ 60 K
EF hand	*PFF0565c*	↑ 60 K
Metabolism		
Glutaredoxin 1	*PFC0271c*	↓ 15, 30 K
ATP-synthase gamma	*PF13_0061*	↓ 30 K
ATP-synthase beta	*PF11_0262*	↓ 30 K
ATP synthase D	*PF13_0227*	↓ 30 K
Apicoplast 1-acyl-sn-glycerol-3-phosphate acyltransferase	*PF14_0421*	↓ 30 K
Malate dehydrogenase	*PF13_0144*	↑ 30 K

Table 2 *continued.*

Protein, by Biological Function	Gene(s)	Regulation Direction, by Radiation Dose[a]
Delta-aminolevulinic acid synthetase (amino transferase)	*PFL2210w*	↑ 30 K
Nucleoside diphosphate kinase	*PFF0275c*	↑ 30 K
Enoyl-ACP reductase	*PFF0730c*	↑ 60 K
Trafficking		
NTF2	*PF14_0228*	↓ 30 K
Synaptobrevin	*MAL13P1.197*	↑ 15 K
Mog1	*MAL13P1.232*	↑ 30 K
SNARE protein	*PF11_0119*	↑ 30 K
Transport		
Mitochondrial carrier protein	*PFI0255c*	↓ 15 K
CorA-Mg2 transporter protein	*MAL13P1.23*	↓ 15 K
CDC50	*PF10_0287*	↓ 30 K
Na^+-dependent Pi transporter	*MAL13P1.206*	↓ 30 K
Surface/exported proteins		
Secreted protein with conserved cysteines	*MAL7P1.14*	↓ 15 K
Sushi repeats	*PFD0295c*	↓ 30 K
Pore-forming toxin domains with a conserved C terminal domain	*MAL13P1.321*	↓ 30 K
RCC1 repeats containing protein	*PFI1500w*	↓ 30 K, 60 K
Erythrocyte membrane protein 3	*PFB0095c*	↓ 60 K
Plasmepsin IX	*PF14_0281*	↑ 30 K
TSP1 domain containing protein	*PFC0210c*	↑ 30 K
VWA	*PF08_0136b*	↑ 30 K
Erythrocyte mem (PfemP)	*PFB0020c*	↑ 30 K
TSP1 domain containing protein	*PFA_0200w*	↑ 30 K, 60 K
VWA and TSP1	*PF13_0201*	↑ 30 K, 60 K
PEPSIN protease	*PFC0495w*	↑ 60 K
UDP-N-acetylglucosamine pyrophosphorylase	*PFE0875c*	↑ 60 K
EGF repeats	*PFL0410w*	↑ 60 K
Lipase (2)		↓ 30 (2) K
PRESAN (2)		↓ 30 (2) K
Rifins (10) (includes stevors)		↓ 30 (1), 60 (1) K; ↑ 15 (1), 30 (6), 60 (1) K
Other signal or transmembrane helix containing proteins (26)		↓ 15 (2), 30 (11), 60 (2) K; ↑ 15 (3), 30 (8), 60 (1) K
Miscellaneous (selected)		
TPR repeat containing protein (3)		↓ 30 (2) K; ↑ 15 (1) K
Beta-propeller repeat containing proteins (2)		↓ 30 (1) K; ↑ 30 (1) K

Abbreviations: K, kilorad of γ-radiation delivered by a Cesium-137 source; ↑, upregulation; ↓, downregulation.

[a] Data denote statistically significant, ≥2-fold increases (↑) or decreases (↓) in the average ratio of gene expression in nonirradiated versus γ-irradiated cultures.

to DNA replication or repair, and interestingly all of them are downregulated. The 5 downregulated genes in our experiments are the origin recognition complex subunit 2 (ORC2) ortholog (PF11_0332), the DNA replication GINS complex protein PSF1 (PFE1175w), one of the replication factor A paralogs (PF11_0332), the topoisomerase II ATPase subunit (PF14_0316), and the Rev1 nucleotidyltransferase (PFI0510c).

Signaling

We found evidence for transcriptional upregulation of certain signaling mechanisms by γ-irradiation (Tables 1 and 2). Of these, the cyclic nucleotide phosphodiesterase (MAL13P1.119) and the EF-hand protein PFF0565c, which is well-conserved across apicomplexan organisms, showed elevated expression. This suggests that the response to γ-irradiation might be channelized via cyclic nucleotide and calcium-dependent signaling networks. Interestingly, we found the protein phosphatase PFI1245c and its activator protein (PF14_0280) to be elevated in expression, whereas 3 protein kinases (MAL7P1.18, PFI0160w, and PFI0100c) were downregulated. Hence, a potential reduction of the specific phosphorylation of proteins might be an aspect of the γ-irradiation response in *P. falciparum*. Both the phosphatidylinositol polyphosphate phosphatase (PF07_0024) and the inositol hexakisphosphate kinase were downregulated, suggesting reduction of inositol phosphate–based signaling in the γ-irradiation response.

A Molecular Signature of γ-Irradiation

Next, on the basis of our microarray data set, we created a molecular signature of γ-radiation–induced transcriptional changes that could be predictive of parasite growth and attenuation. Real-time PCR was performed in triplicate on pooled RNA isolated from untreated or γ-radiation–treated (60 K) parasite cultures on the following functionally diverse genes: protein phosphatase β (PFI1245c), OTU-like cysteine protease (PFI1135c), nucleolar preribosomal GTPase (PFE1435c), 40S ribosomal protein S7 (PF13_0014), AAA ATPase (PFI0355c), and RNA pseudouridylate synthase (PFL1350w). We found

Table 3. Molecular Signature of γ-Irradiation in Asexual Blood-Stage *Plasmodium falciparum*

Gene	Description	Microarray[a]	Real-Time PCR[a]	Biological Function
PFI1245c	Protein phosphatase β	2.06 ± 0.05	1.70 ± 0.28	Signal transduction
PFI1135c	OTU-like cysteine protease	−2.05 ± 0.10	−1.86 ± 0.10	Ubiquitin and proteasome
PFE1435c	Nucleolar preribosomal GTPase	−2.19 ± 0.12	−1.70 ± 0.06	Translation
PF13_0014	40S ribosomal protein S7	−2.20 ± 0.06	−2.04 ± 0.20	Translation
PFI0355c	AAA ATPase	−2.30 ± 0.04	−1.39 ± 0.13	Chaperone/protein stability
PFL1350w	RNA pseudouridylate synthase	−2.50 ± 0.07	−1.81 ± 0.28	Translation

Abbreviations: K, kilorad of γ-radiation delivered by a Cesium-137 source; PCR, polymerase chain reaction.

[a] Performed in RNA samples prepared from asynchronous *P. falciparum* parasites irradiated at 60 K.

that measurements of changes in messenger RNA (mRNA) abundance by real-time PCR were in accordance with our microarray results (Table 3).

DISCUSSION

In this article, we provide the first comprehensive study on survival and growth and examine the molecular and cellular alterations in intraerythrocytic *P. falciparum* treated with high doses of γ-radiation. Exposure to high doses of γ-radiation causes the attenuation and eventual death of intraerythrocytic *P. falciparum*. At 72 hours after treatment with 60 K of γ-radiation, a 99.5% reduction in parasitemia was observed (Figure 1). However, the parasites that survived the irradiation treatment had a normal growth profile, suggesting that these parasites arose from a few parasite clones that were either unaffected by γ-irradiation or were able to repair the damage and repopulate.

The mechanism of cell death in *Plasmodium* parasites is poorly understood. For example, apoptosis, a form of programmed cell death, while common in eukaryotic cells, has never been conclusively demonstrated in asexual-stage *Plasmodium* parasites [23]. In this study, we failed to observe any DNA fragmentation, a hallmark of cell death, using terminal deoxynucleotidyl transferase–mediated dUTP-biotin nick end labeling (TUNEL) analysis in *P. falciparum* 2 hours after treatment with 60 K of γ-radiation (data not shown). Previously, the presence of TUNEL-positive *P. falciparum* was reported following treatment at 41°C for 2 hours [18].

Interestingly, we noted a delay of 24–48 hours before a significant decline in parasitemia in γ-radiation–treated parasites, raising the prospect that, prior to clearance, these parasites might have undergone mitotic catastrophe or senescence. The fact that γ-radiation–treated parasites had significantly fewer distinguishable nuclei per parasite suggested that the cycle of nuclear duplication was perturbed (Figure 2*C* and 2*E*, DAPI). γ-irradiation also had an adverse effect on parasite organogenesis and maturation. Irradiated cultures contained fewer RAP1-positive (Figure 2*C*) and EBA 175–positive parasites, indicating that rhoptry and microneme organelle formation may have been disrupted in these parasites (Figure 2*E*). Electron microscopy further revealed irradiation-associated structural abnormalities, such as sparse cytoplasms, reduced numbers of ribosomes, disorganized organelles, and, in some instances, large vacuoles (Figure 3*B* and 3*D*). While the observation of parasites with fewer nuclei on average may be indicative of mitotic catastrophe, the general disorder of organelles within the cytoplasm and the degree of cell and organelle swelling suggest that these parasites were progressing toward cell death. This interpretation is consistent with a published guideline defining stressed cells in higher eukaryotes [24].

We also performed the first in-depth molecular characterization of the irradiation response at the transcriptional level in *P. falciparum* that were treated with sublethal (15 K and 30 K) and lethal (60 K) doses of γ-radiation, and we created a molecular signature of γ-radiation–induced parasite growth attenuation by validating the microarray transcriptional changes of 6 novel biomarkers by real-time PCR. The significance of this signature is evident by the demonstrated role of *Pf* AAA ATPase in parasite cell death [25] and of *Pf* RNA pseudouridylate synthase in parasite growth attenuation [26].

A major effect of γ-irradiation treatment was a general downregulation of the parasite translation machinery (Tables 1 and 2). One such molecule with reduced transcription in response to irradiation was a ribosomal RNA–modifying pseudouridylate synthase. It was recently shown that a pseudouridine synthase is critical for stage conversion of tachyzoites to bradyzoites in *Toxoplasma gondii* [27]. Similarly, disruption of at least 1 *P. falciparum* pseudouridylate synthase results in a 47% attenuation of the parasite in in vitro cultures [26]. Hence, the pseudouridylate synthase recovered in this study might be an attractive target for development of mutant attenuated parasites.

One of the few genes related to RNA metabolism that was upregulated by irradiation (2.15 ± 0.06-fold in response to a 30-K dose) encoded *Pf* LSM12, an Sm superfamily protein with a functional link to translational arrest. LSM12 is a component of stress granules [28], which are composed of repositories of untranslated mRNAs and 40S ribosomal subunits that form during cellular stress [29, 30]. We propose that

γ-irradiation may result in translational arrest with a concomitant accumulation of untranslated mRNAs that may accumulate in stress granules in conjunction with the *Pf* LSM12 protein.

Another major effect of γ-irradiation is the downregulation of genes directly related to the DNA replication machinery of *P. falciparum* (Tables 1 and 2). Among these, of particular interest is *Pf* topoisomerase II. Expression and activity of *Pf* topoisomerase II peaks during the trophozoite/schizont stage when DNA replication occurs [31], and the cleavage site of *Pf* topoisomerase II is a highly AT-rich element (approximately 97%) present once per chromosome that has previously been proposed as the site of the parasite centromere [32]. Proliferation of parasites is inhibited by antisense oligonucleotides against the *Pf* topoisomerase II gene, indicating the importance of this molecule in parasite growth [33]. The downregulation of the Rev1 ortholog is also of considerable interest because it is a key nucleotidyltransferase that is involved in repair of abasic lesions via template-independent addition of dCMP [34]. The downregulation of the DNA replication genes could be a part of the general regression of growth and proliferation, a hypothesis further supported by the modulation of translation-related genes observed in our experiments.

A matter of concern in terms of the safety of γ-radiated vaccines might be that, in our data set, we observed a large set of genes pertaining to cell-surface interactions, host cell remodeling, and secreted proteins being both downregulated and upregulated (eg, rifins, plasmepsin IX, and Rex2; Tables 1 and 2). These alterations might result in parasites with different adhesive and host interaction capabilities whose pathological properties remain unclear.

The results reported here provide a platform for further defining the mechanism of γ-radiation–induced attenuation and cell death and the associated biomarkers of parasite attenuation and virulence.

Supplementary Data

Supplementary materials are available at *The Journal of Infectious Diseases* online (http://jid.oxfordjournals.org/). Supplementary materials consist of data provided by the author that are published to benefit the reader. The posted materials are not copyedited. The contents of all supplementary data are the sole responsibility of the authors. Questions or messages regarding errors should be addressed to the author.

Notes

Acknowledgments. We thank Dr Anthony Holder, for providing the anti-RAP1 mAb 7H8/50, and Ms Yukiko Kozakai, for help with statistical analysis.

Financial support. This work was supported by the intramural grants from the Food and Drug Administration and National Institutes of Health.

Potential conflicts of interest. All authors: No reported conflicts.

All authors have submitted the ICMJE Form for Disclosure of Potential Conflicts of Interest. Conflicts that the editors consider relevant to the content of the manuscript have been disclosed.

References

1. Eriksson D, Stigbrand T. Radiation-induced cell death mechanisms. Tumour Biol **2010**; 31:363–72.
2. Ellis RW. Elsevier Health Sciences. London **2008**:1335–56.
3. Osterholm MT, Norgan AP. The role of irradiation in food safety. N Engl J Med **2004**; 350:1898–901.
4. Nussenzweig RS, Vanderberg J, Most H, Orton C. Protective immunity produced by the injection of x-irradiated sporozoites of *Plasmodium berghei*. Nature **1967**; 216:160–2.
5. Rieckmann KH, Beaudoin RL, Cassells JS, Sell KW. Use of attenuated sporozoites in the immunization of human volunteers against falciparum malaria. Bull World Health Organ **1979**; 57(Suppl 1): 261–5.
6. Vanderberg JP. Reflections on early malaria vaccine studies, the first successful human malaria vaccination, and beyond. Vaccine **2009**; 27:2–9.
7. Singh R, George J, Shukla Y. Role of senescence and mitotic catastrophe in cancer therapy. Cell Div **2010**; 5:4.
8. Jonathan EC, Bernhard EJ, McKenna WG. How does radiation kill cells? Curr Opin Chem Biol **1999**; 3:77–83.
9. Hartwell LH, Weinert TA. Checkpoints: controls that ensure the order of cell cycle events. Science **1989**; 246:629–34.
10. Bucher N, Britten CD. G2 checkpoint abrogation and checkpoint kinase-1 targeting in the treatment of cancer. Br J Cancer **2008**; 98:523–8.
11. Gerald NJ, Majam V, Mahajan B, Kozakai Y, Kumar S. Protection from experimental cerebral malaria with a single dose of radiation-attenuated, blood-stage *Plasmodium berghei* parasites. PLoS One **2011**; 6:e24398.
12. Suzuki M, Waki S, Igarashi I, Takagi T, Miyagami T, Nakazawa S. An alternative approach to malaria vaccine with a permanent attenuated mutant from a high virulence *Plasmodium berghei* strain. Zentralbl Bakteriol Mikrobiol Hyg A **1987**; 264:319–25.
13. Sadun EH, Wellde BT, Hickman RL. Resistance produced in owl monkeys (*Aotus trivirgatus*) by inoculation with irradiated *Plasmodium falciparum*. Mil Med **1969**; 134:1165–75.
14. Epstein JE, Tewari K, Lyke KE, et al. Live attenuated malaria vaccine designed to protect through hepatic CD8 T cell immunity. Science **2011**; 334:475–80.
15. Chattopadhyay R, Conteh S, Li M, James ER, Epstein JE, Hoffman SL. The effects of radiation on the safety and protective efficacy of an attenuated *Plasmodium yoelii* sporozoite malaria vaccine. Vaccine **2009**; 27:3675–80.
16. Hoffman SL, Billingsley PF, James E, et al. Development of a metabolically active, non-replicating sporozoite vaccine to prevent *Plasmodium falciparum* malaria. Hum Vaccin **2010**; 6:97–106.
17. Agnandji ST, Lell B, Soulanoudjingar SS, et al. First results of phase 3 trial of RTS,S/AS01 malaria vaccine in African children. N Engl J Med **2011**; 365:1863–75.
18. Oakley MS, Kumar S, Anantharaman V, et al. Molecular factors and biochemical pathways induced by febrile temperature in intraerythrocytic *Plasmodium falciparum* parasites. Infect Immun **2007**; 75:2012–25.
19. Oakley MS, McCutchan TF, Anantharaman V, et al. Host biomarkers and biological pathways that are associated with the expression of experimental cerebral malaria in mice. Infect Immun **2008**; 76:4518–29.
20. Oakley MS, Anantharaman V, Venancio TM, et al. Molecular correlates of experimental cerebral malaria detectable in whole blood. Infect Immun **2011**; 79:1244–53.
21. Cowman AF, Crabb BS. Invasion of red blood cells by malaria parasites. Cell **2006**; 124:755–66.

22. Margos G, Bannister LH, Dluzewski AR, Hopkins J, Williams IT, Mitchell GH. Correlation of structural development and differential expression of invasion-related molecules in schizonts of *Plasmodium falciparum*. Parasitology **2004**; 129:273–87.
23. Totino PR, Daniel-Ribeiro CT, Corte-Real S, de Fatima Ferreira-da-Cruz M. *Plasmodium falciparum*: erythrocytic stages die by autophagic-like cell death under drug pressure. Exp Parasitol **2008**; 118: 478–86.
24. Kroemer G, Galluzzi L, Vandenabeele P, et al. Classification of cell death: recommendations of the Nomenclature Committee on Cell Death 2009. Cell Death Differ **2009**; 16:3–11.
25. Rathore S, Jain S, Sinha D, et al. Disruption of a mitochondrial protease machinery in *Plasmodium falciparum* is an intrinsic signal for parasite cell death. Cell Death Dis **2011**; 2:e231.
26. Balu B, Singh N, Maher SP, Adams JH. A genetic screen for attenuated growth identifies genes crucial for intraerythrocytic development of *Plasmodium falciparum*. PLoS One **2010**; 5:e13282.
27. Anderson MZ, Brewer J, Singh U, Boothroyd JC. A pseudouridine synthase homologue is critical to cellular differentiation in *Toxoplasma gondii*. Eukaryot Cell **2009**; 8:398–409.
28. Swisher KD, Parker R. Localization to, and effects of Pbp1, Pbp4, Lsm12, Dhh1, and Pab1 on stress granules in *Saccharomyces cerevisiae*. PLoS One **2010**; 5:e10006.
29. Bond U. Stressed out! Effects of environmental stress on mRNA metabolism. FEMS Yeast Res **2006**; 6:160–70.
30. Buchan JR, Parker R. Eukaryotic stress granules: the ins and outs of translation. Mol Cell **2009**; 36:932–41.
31. Cheesman S, Horrocks P, Tosh K, Kilbey B. Intraerythrocytic expression of topoisomerase II from *Plasmodium falciparum* is developmentally regulated. Mol Biochem Parasitol **1998**; 92:39–46.
32. Kelly JM, McRobert L, Baker DA. Evidence on the chromosomal location of centromeric DNA in *Plasmodium falciparum* from etoposide-mediated topoisomerase-II cleavage. Proc Natl Acad Sci USA **2006**; 103:6706–11.
33. Noonpakdee W, Pothikasikorn J, Nimitsantiwong W, Wilairat P. Inhibition of *Plasmodium falciparum* proliferation in vitro by antisense oligodeoxynucleotides against malarial topoisomerase II. Biochem Biophys Res Commun **2003**; 302:659–64.
34. Lawrence CW. Cellular functions of DNA polymerase zeta and Rev1 protein. Adv Protein Chem **2004**; 69:167–203.